RNA functional control by hydrolysis reversible acylation

Abstract

We present the hydrolysis reversible acylation of RNA 2′-OH for functional control. Compared with previously reported acylating reagents, our new molecule **EST1A** eliminated the need of toxic organic molecules in deacylation. Instead, the acylation was removed by biocompatible intracellular stimuli such as esterase and histidine. After validating the reversibility using oligonucleotides, we applied our acylating reagent on functional RNAs, including broccoli aptamer, eGFP mRNA, and eGFP siRNA, and gained activity control on them. Further inhibitory and enhancive assays in HepG2 and U87MG cells confirmed that both carboxylesterase and cholinesterase contributed to deacylation *in cellulo*. By taking advantage of differences in esterase expression among cell lines, our new strategy can benefit the development of cell-selective gene therapeutics.

RNA is a multi-functional biomacromolecule. It participates in biochemical reactions such as protein synthesis, expression regulation, and RNA modification.[1-4] Due to its versatility, RNA has been indispensable in both research and therapeutic scenarios.[5-8] The great potential of RNA in these fields has stimulated the development of methods for activity control, interrogation of biological roles, and labeling.[9-13] Previous work has revealed the effectiveness of reversible 2′-OH in modulating RNA functionality.[14-17] RNAs are deactivated after acylation (e.g., the mRNA cannot be translated) but can be reactivated via deacylation.[16] Moreover, as a type of post-synthetic modification, 2′-OH acylation can modify not only short oligonucleotides but also long and

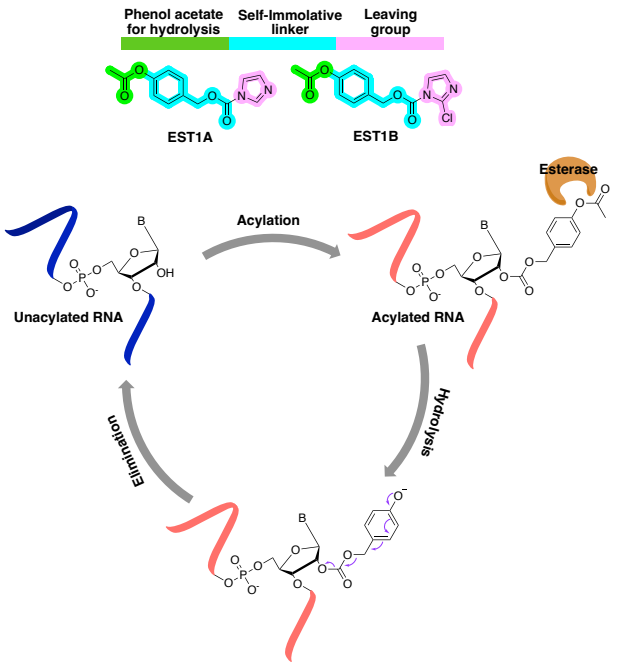

Scheme 1. Design principle of acylating molecules and proposed mechanism of reversible acylation.

structured RNAs.[18, 19] However, the current deacylation methods require toxic organic molecules or UV light, significantly restricting its therapeutic potential.[16, 17, 20]

To eliminate the cytotoxicity at the deacylation step, we incorporated a hydrolysis-responsive ester bond in the acylating reagent. As the ester bond is liable in the cellular environment due to the presence of esterase, we envisioned that the function of acylated RNA could be gradually restored via deacylation *in the cellulo*.[21-23] In this work, we selected carboxylesterase and cholinesterase as enzymes of interest. Carboxylesterase (CES) digests esters; therefore, it is closely related to energy products for cells.[24] Previous research also showed that CES was overexpressed in cancer cells and contributed to tumor migration.[25-29] Cholinesterase, on the other hand, is crucial in the neuro system. It breaks down the neurotransmitters so that cholinergic neurons can return to their resting state.[30] The abnormal activity of cholinesterase can cause miscommunication among cells and may lead to Alzheimer's disease.[31] Besides esterase, we also discovered that imidazole and its amino acid derivative, histidine, could initiate the hydrolysis of the ester bond and recover the RNA 2′-OH. Due to the difference in the levels of these intracellular stimuli among cell lines, the restoration rate of RNA also varies. Therefore, cell-specific therapy using RNA-based drugs can be achieved.

We designed two molecules for our hydrolysis reversible strategy. Due to the high efficiency in previous literature, imidazole and 2-chloroimidazole were incorporated as the leaving group for our acylating reagents (**Scheme 1**, see **Scheme S1** for synthetic routes).[15, 17] The benzyl acetate group was introduced for hydrolysis responsiveness. The benzyl phenol intermediate formed in

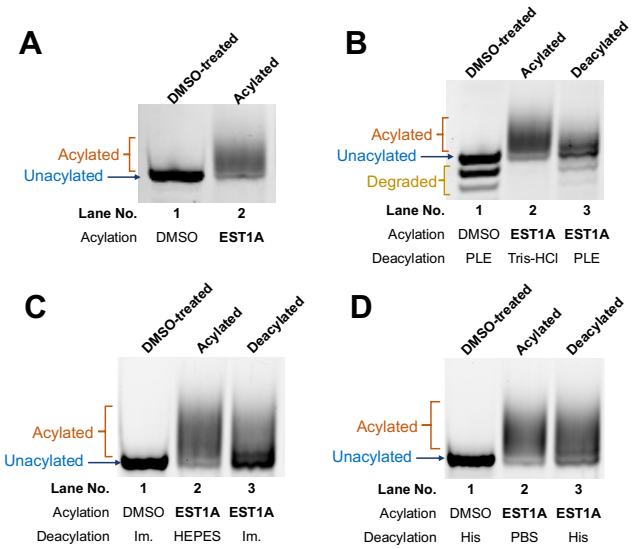

Figure 1. Reversible acylation of Cy3-U_{16} RNA. Samples analyzed by 30% denaturing PAGE (monomer ratio: 19:1). **A**) 120 nM oligonucleotides treated with 10% DMSO or 100 mM **EST1A** at 37 °C for 4 h. **B**) Removal of acylation by 40 U/mL porcine liver esterase in 50 mM Tris-HCl (pH 8.0). Degradation caused by RNase in the enzyme sample. **C**) Removal of acylation by 50 mM imidazole in 50 mM HEPES buffer (pH 7.5). **D**) Removal of acylation by 50 mM histidine in 1× PBS buffer (pH 7.4).

ester hydrolysis would undergo 1,6-elimination. After quinomethide and carbon dioxide were released (**Scheme 1**), the 2′-OH could be recovered.

We first tested the acylating reactivity of the **EST1A** molecule using a 5′-Cy3-tagged RNA oligonucleotide that consists of 16 uridines (Cy3-U_{16}). 120 nM Cy3-U_{16} RNA was treated with 1.0 M **EST1A** or 10% DMSO at 37 °C for 4 hours. Both samples were then analyzed by 30% denaturing polyacrylamide gel electrophoresis (monomer ratio 19:1) and imaged in the Cy3 channel. We observed shifted bands from lane 2 in gel image **Figure 1A**, indicating the higher molecular weight from successful acylation. As for **EST1B**, though bearing a more reactive leaving group, it did not induce acylation under all the tested conditions (**Figure S1**). The restricted acylation might be attributed to its low solubility or fast hydrolysis.[15]

Next, the reversal of the acylation by esterase was investigated. We acylated Cy3-U_{16} by incubating it with 50 mM **EST1A** at 37 °C for 6 hours (**Figure S3**). The acylated RNA was treated with porcine liver esterase (PLE) or Tris-HCl buffer. The DMSO-treated RNA was used as the control. As the PAGE analysis shows (**Figure 1B** and **Figure S4A**), we observed that bands from lane 3 (deacylated RNA) were less shifted than those from lane 2 (acylated RNA), suggesting the removal of acylation by PLE.

While optimizing acylation conditions for **EST1A**, we observed that incubation with a longer time and a high concentration of acylating reagents resulted in a lower yield of acylated RNA (**Figure S2** and **S3**). We hypothesized that the imidazole formed via acylation and hydrolysis could initiate deacylation. In fact, imidazole was reported as a catalyst of ester hydrolysis.[32] To test our theory, we treated the acylated RNA oligonucleotide with 25 mM imidazole and analyzed the samples by denaturing PAGE. We discovered that imidazole effectively removed the acylation within 30 minutes at 37 °C (**Figure S4B**). To eliminate the influence of pH, we repeated the deacylation in the 50 mM HEPES buffer (pH 7.5), and the disappearance of shifted bands from lane 3 in **Figure 1C** (also see **Figure S4C**) supported our hypothesis. Inspired by imidazole, we then investigated the deacylation by histidine – an amino acid that bears an imidazole ring as its side branch. The disappearance of shifted bands from lane 3 in **Figure 1D** (also see **Figure S4D**) indicated that histidine was also a potent deacylating reagent.

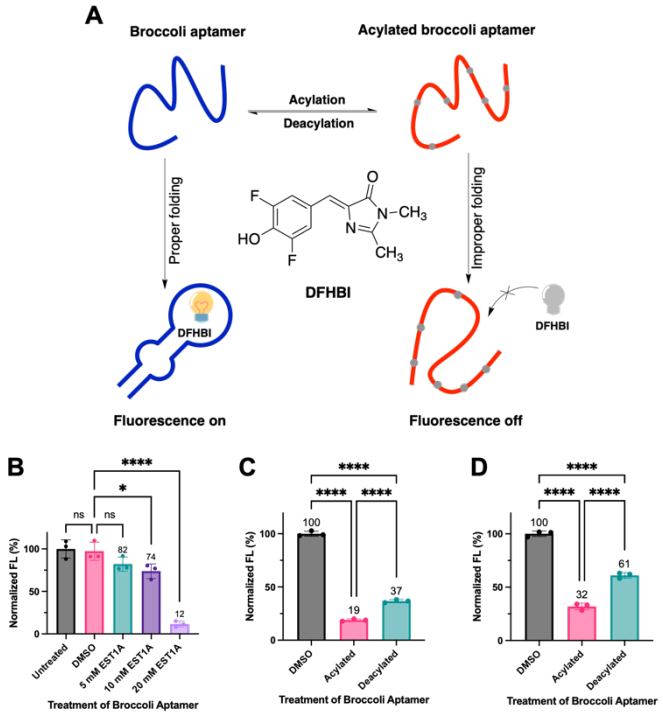

Figure 2. **A**) Modulation of aptamer-DFHBI interaction by reversible acylation. **B**) Fluorescence of DFHBI binding to broccoli aptamer acylated with increasing amounts of **EST1A** in 10% DMSO at 37 °C for 4 h. **C**) Restoration of aptamer-DFHBI interaction by 50 mM histidine in HEPES buffer. **D**) Restoration of aptamer-DFHBI interaction by 50 mM imidazole in PBS buffer. Broccoli aptamer acylated by 20 mM **EST1A** in 10% DMSO at 37 °C for 4 h For quantitative analysis, the error bar represents the standard deviation (n=3). T-test: ns, $P > 0.05$; *, $P \leqslant 0.05$; **, $P \leqslant 0.01$; ***, $P \leqslant 0.001$; ****, $P \leqslant 0.0001$.

After validating the reversibility of our acylating reagent using short oligonucleotides, we turned to the folding control of longer RNAs by **EST1A** molecule. We use the F-30 broccoli aptamer as the model. The properly folded F-30 broccoli aptamer can bind with the DFHBI molecule, and by restricting the intramolecular movement, the aptamer-DFHBI system could emit fluorescence.[33, 34] The acylation on the aptamer prevented it from folding properly, thereby disrupting the aptamer-DFHBI interaction and turning off the fluorescent signal (**Figure 2A**). We incubated 1.5 μg of F-30 broccoli aptamer with DMSO or increasing concentrations of **EST1A**. After isolation by EtOH precipitation, the aptamer was folded in the HEPES folding buffer, followed by the addition of DFHBI (20 equiv.). Weaker fluorescent signals were recorded from aptamers acylated by higher concentrations of **EST1A** (**Figure 2B**); hence, we confirm that **EST1A** disrupted the aptamer-DFHBI interaction. The study of deacylation was followed. We incubated acylated aptamer with 50 mM histidine in PBS buffer (pH 7.4) and recovered 37% relative fluorescence intensity (**Figure 2C**), which was almost twice the intensity of the one incubated without histidine (19%). The acylation could be removed by imidazole as well. By treating the acylated aptamer with imidazole in HEPES buffer (50 mM, pH 7.5), we recovered 61% of relative fluorescence intensity (**Figure 2D**), which was significantly higher than fluorescence from acylated aptamer (32%). The RNA folding pattern in different buffers may cause the variance of deacylation efficiency between

histidine and imidazole. Since the broccoli aptamer eventually folded and incubated in the HEPES buffer, the acylated aptamer in the HEPES buffer was more likely to adopt a similar structure that favored the folding. The restoration of the fluorescence signal from the F-30 broccoli aptamer-DFHBI system proved that our reversible acylation strategy can be utilized to control the folding of RNA.

Next, we utilize our acylating reagent to control the translation of mRNA coding for enhanced green fluorescence protein (eGFP). As previously reported, the acylation at 2′-OH could interfere with the reading of mRNA by the ribosome and thus inhibit protein synthesis (**Figure 3A**). To test its ability for gene expression control, we acylated 40 ng/μL eGFP mRNA with 5 mM **EST1A** at 37 °C for 4 h. For deacylation, the acylated mRNA was precipitated and then treated with 50 mM histidine or imidazole in the corresponding buffer at 37 °C for 4 h. Finally, mRNA was transfected into HepG2 cells by lipofectamine MessengerMax, and the green fluorescence was measured after overnight incubation. The translation of eGFP mRNA was suppressed by acylation (**Figure 3B**, **S5**): we only detected 20% relative fluorescence intensity from HepG2 cells transfected with acylated eGFP mRNA. For cells transfected by mRNA that was deacylated by histidine in the PBS buffer, we observed comparable green fluorescence intensity (71%) to cells transfected with DMSO-treated control (**Figure 3B**, **3C**, and **S5A**). Imidazole was also able to restore the translation of acylated mRNA, but the recovery rate was significantly lower: cells transfected with eGFP mRNA deacylated by imidazole in HEPES buffer only showed 31% relative fluorescence intensity (**Figure 3C** and **S5B**). By applying the **EST1A** molecule to eGFP mRNA, we gained

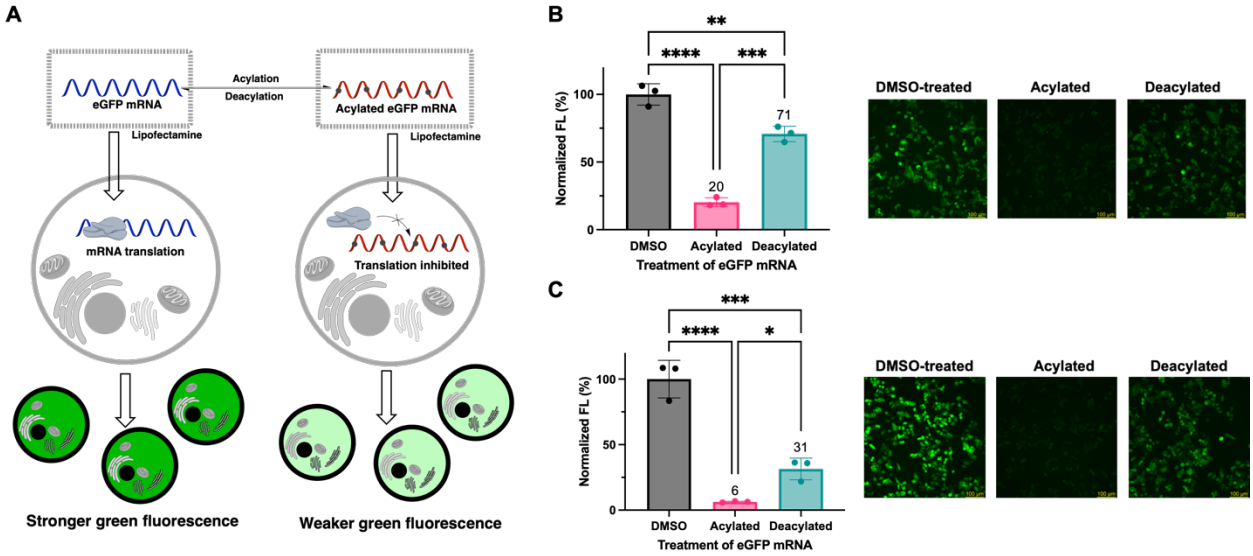

Figure 3. **A**) Modulation of eGFP mRNA translation by reversible acylation. **B**) Quantitative analysis for and functional restoration of eGFP mRNA by 50 mM histidine. Image of HepG2 cells transfected with DMSO-treated, acylated, and deacylated eGFP mRNA. **C**) Quantitative analysis for and functional restoration of eGFP mRNA by 50 mM imidazole. Image of HepG2 cells transfected with DMSO-treated, acylated, and deacylated eGFP mRNA. eGFP mRNA acylated by 5 mM **EST1A** in 10% DMSO at 37 °C for 4 h. For quantitative analysis, the error bar represents the standard deviation (n=3). T-test: ns, $P > 0.05$; *, $P \leqslant 0.05$; **, $P \leqslant 0.01$; ***, $P \leqslant 0.001$; ****, $P \leqslant$

control of gene expression and established that the reversible acylation method was compatible with long and structured mRNA.

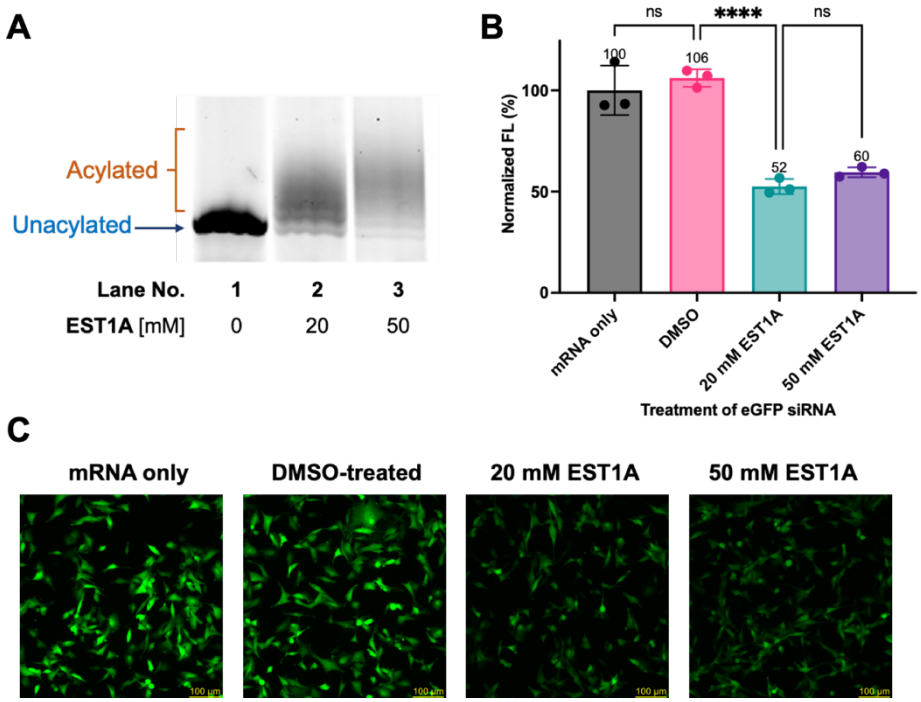

Figure 4. *In vitro* acylation of eGFP siRNA (single-stranded). **A**) 30% denaturing PAGE analysis of DMSO-treated and acylated eGFP siRNA (single-stranded). Gel stained by SYBR-gold. **B**) Quantitative analysis of GFP fluorescence intensity from U87MG cells co-transfected with eGFP mRNA and eGFP siRNAs subjected to different treatments. The error bar represents the standard deviation (n=3). T-test: ns, $P > 0.05$; *, $P \leq 0.05$; **, $P \leq 0.01$; ***, $P \leq 0.001$; ****, $P \leq 0.0001$. **C**) Images of cells co-transfected with eGFP mRNA and eGFP siRNAs subjected to different treatments.

Due to the susceptibility of broccoli aptamer and mRNA toward the RNase (**Figure S8** and **S9**), we turned to single-stranded siRNA as the model for the study of functional control by porcine liver esterase.[35, 36] We prepared DMSO-treated and acylated eGFP siRNAs and analyzed them using PAGE, as shown in **Figure 4A**. The eGFP siRNAs were then co-transfected with eGFP mRNA by lipofectamine MessengerMax into U87MG cells.[37] We first expected the acylation would hinder the binding of siRNA to its mRNA target; hence, the acylated siRNA would be less efficient in gene knockdown.[38] However, the results were contradictory to our expectations. We observed no significant gene knockdown for DMSO-treated siRNA but efficient translational suppression for acylated siRNA (**Figure 4B**, **4C**, and **S6**). The fluorescence was suppressed to 52% and 60% when acylated by 20 mM and 50 mM **EST1A**. The inefficient gene knockdown of unacylated siRNA may be attributed to an insufficient amount. As for unexpected translational suppression by acylated siRNA, we believed that, by increasing the lipophilicity of the RNA strand, the acylation facilitated the membrane penetration and endosomal escape.[39, 40] Upon the arrival of

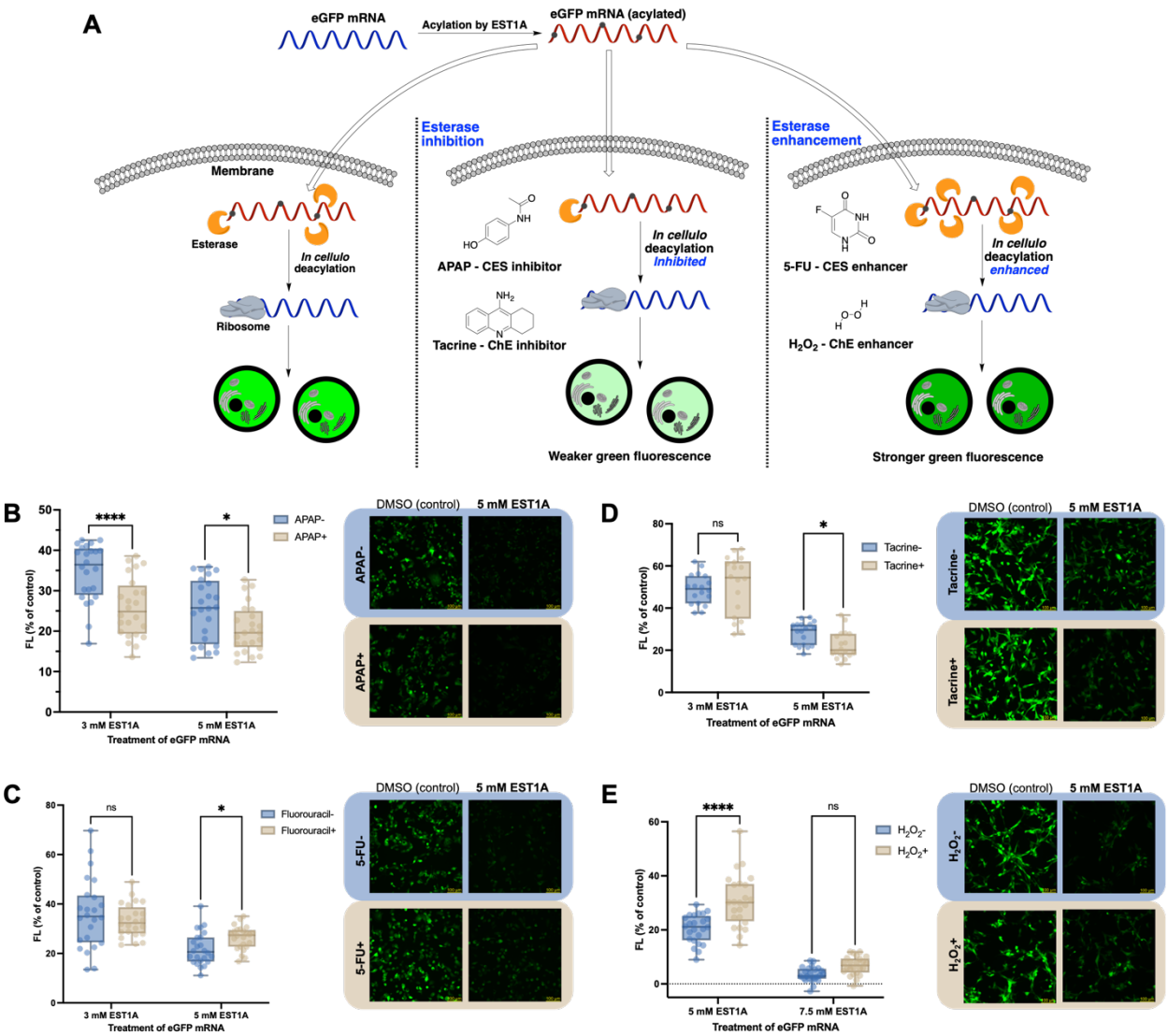

Figure 5. A) Modulation of cellular enzyme activity and deacylation efficiency. The inhibition of enzymes leads to weaker fluorescence signals and vice versa. **B)-D**) Quantitative analysis of fluorescence intensity and images from cells transfected with DMSO-treated or **EST1A**-acylated eGFP mRNA. For quantitative analysis, the average of fluorescence intensities from cells transfected with DMSO-treated mRNA was set to 100%. n=24, t-test: ns, $P > 0.05$; *, $P \leqslant 0.05$; **, $P \leqslant 0.01$; ***, $P \leqslant 0.001$; ****, $P \leqslant 0.0001$.

the cytoplasm, the acylated siRNA may still stop the codon reading by the ribosome despite the mismatch.[41] Alternatively, siRNA could undergo deacylation in the cytoplasm and then induce mRNA degradation via the RNAi pathway.[42] Though unanticipated, we concluded that our acylating reagent can enhance the inhibitory effects of siRNA.

We were then curious to see if the cellular esterase induced the removal of acylation and restored the RNA function *in cellulo*. For visualization purposes, we selected eGFP mRNA again and acylated it with DMSO (control) or **EST1A**. For carboxylesterase, we treated HepG2 cells with hepatotoxic drug acetaminophen (APAP) for inhibition and anticancer drug 5-fluorouracil (5-FU) for enhancement (**Figure 5A**).[43-49] The eGFP mRNAs were then transfected to HepG2 cells

subjected to different treatments. As shown in **Figure 5B**, APAP decreased the carboxylesterase activity and suppressed the *in cellulo* deacylation. We observed drops in relative fluorescence intensity: 34.6% to 25.8% for 3 mM **EST1A**-acylated mRNA and 25.3% to 20.6% for 5 mM **EST1A**-acylated mRNA (see **Figure S7A** as well). For the enhancive assay, we treated the HepG2 cells with 80 μM 5-fluorouracil (5-FU) prior to the mRNA transfection. As shown in **Figure 5C** and **S7B**, when eGFP mRNA was acylated by 5 mM **EST1A**, HepG2 cells exposed to 5-FU exhibited stronger relative fluorescence signals (26.2%) than those without 5-FU exposure (21.9%). Next, we investigated the deacylation by cholinesterase. We chose U87MG cells and inhibited its cellular cholinesterase by 50 μM tacrine.[50, 51] The tacrine-treated U87MG cells showed lower relative fluorescence intensity (22.5%) compared with untreated cells (28.1%) when transfected with 5 mM **EST1A**-acylated mRNA, indicating the *in cellulo* deacylation was suppressed (**Figure 5D** and **S7C**). For the enhancive assay, we treated the U87MG cells with 200 μM hydrogen peroxide for 1 hour before mRNA transfection. Oxidation stress can increase cholinesterase in neuron cells; therefore, it should favor the *in cellulo* deacylation.[52] Cells without the treatment of H_2O_2 showed 20.5% relative fluorescence intensity (acylated mRNA acylated by 5 mM **EST1A**), whereas the oxidation stress promoted the intensity to 30.6% (**Figure 5E** and **S7D**). By modulating the cellular activity of esterase, we confirmed that both carboxylesterase and cholinesterase participated in the acylation removal *in cellulo*.

The *in cellulo* activation of eGFP mRNA showed the promise of our approach in developing cell-selective RNA-based drugs. However, for therapeutic purposes, we need to ensure that the modification and/or the deacylation product does not exert cytotoxicity. Indeed, research has revealed severe toxicity of RNA-based drugs coming from unexpected interactome.[53, 54] In our case, the quinone methide side product from deacylation may act as a Michael acceptor, crosslinking with nucleophiles from biomolecules.[55, 56] To test the viability, we use the C_{12}-Resazurin and SYTOX Green stain. Live cells can reduce C_{12}-Resazurin and yield a red product with strong emission at 575 nm. Meanwhile, SYTOX Green cannot penetrate intact cell

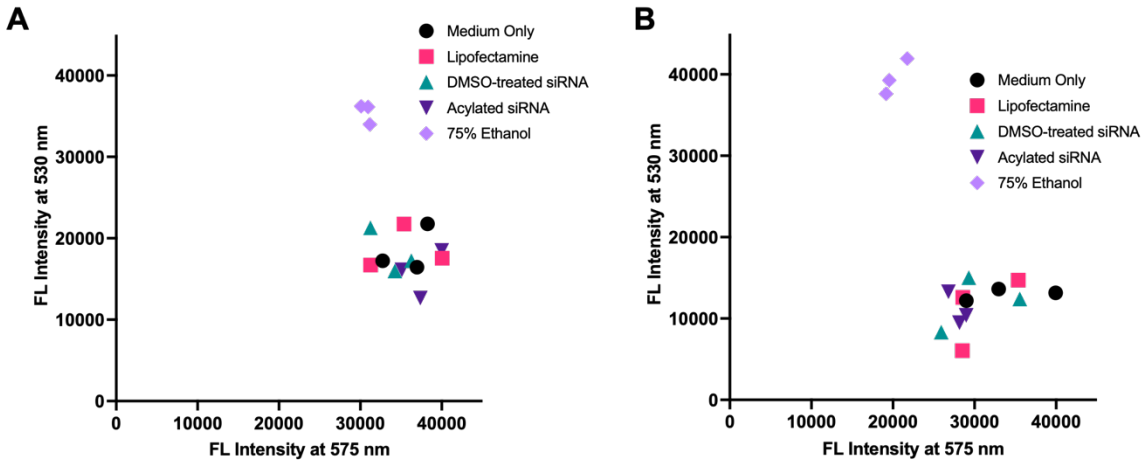

Figure 6. Viability test of HepG2 (**A**) and U87MG (**B**) cells using the LIVE/DEAD Cell Vitality Kit. For dead cell control, cells were treated with 100 μL/well 75% EtOH at 37 °C for 20 min.

membranes; thus, its emission (530 nm) should be weak for live cells. As **Figure 6** shows, in both U87MG and HepG2 cell lines, cells treated with only medium, lipofectamine, unacylated RNA, and acylated RNA all exhibit strong fluorescence at 575 nm and weak fluorescence at 530 nm, suggesting the low cytotoxicity of acylation on the RNA. Additional MTT assay also confirms minimal (**Figure S10**) toxicity from the acylation.

In this report, we developed the **EST1A** molecule for the strategy of hydrolysis reversible acylation on RNA 2′-OH. After treating with porcine liver esterase, histidine, or imidazole, the acylations on the oligonucleotide could be efficiently removed. We then turned to the function control of longer RNAs. The activities of acylated broccoli aptamer and eGFP mRNA were restored when incubated with histidine and imidazole. The acylating reagent was next tested on single-stranded siRNA by co-transfection with eGFP mRNA into HepG2 cells. Surprisingly, the acylated siRNA exhibited higher gene knockdown efficiency than the unacylated one, probably due to the increased cellular uptake or mismatch tolerance. Furthermore, we investigated the *in cellulo* deacylation of eGFP mRNA by intracellular esterases. We observed a positive correlation between fluorescence restoration and esterase activity by regulating the carboxylesterase in HepG2 cells and cholinesterase in U87MG cells. Such results proved the participation of these enzymes in the acylation reversal. Finally, from the cytotoxicity assay, we did not detect significant toxicity from the acylation itself. We believe our hydrolysis reversible acylation provides a new type of modification for RNA-based drugs to achieve cell-selective therapy in the future.

References:

(1) Ulveling, D.; Francastel, C.; Hubé, F. When one is better than two: RNA with dual functions. *Biochimie* **2011**, *93* (4), 633-644. DOI: https://doi.org/10.1016/j.biochi.2010.11.004.
(2) Roden, C.; Gladfelter, A. S. RNA contributions to the form and function of biomolecular condensates. *Nature Reviews Molecular Cell Biology* **2021**, *22* (3), 183-195.
(3) Chen, L.-L. The expanding regulatory mechanisms and cellular functions of circular RNAs. *Nature reviews Molecular cell biology* **2020**, *21* (8), 475-490.
(4) Assmann, S. M.; Chou, H.-L.; Bevilacqua, P. C. Rock, scissors, paper: How RNA structure informs function. *The Plant Cell* **2023**, *35* (6), 1671-1707. DOI: 10.1093/plcell/koad026 (acccessed 3/14/2024).
(5) Belancio, V. P. Importance of RNA analysis in interpretation of reporter gene expression data. *Analytical Biochemistry* **2011**, *417* (1), 159-161. DOI: https://doi.org/10.1016/j.ab.2011.05.035.
(6) Zhu, Y.; Zhu, L.; Wang, X.; Jin, H. RNA-based therapeutics: an overview and prospectus. *Cell Death & Disease* **2022**, *13* (7), 644. DOI: 10.1038/s41419-022-05075-2.
(7) Winkle, M.; El-Daly, S. M.; Fabbri, M.; Calin, G. A. Noncoding RNA therapeutics — challenges and potential solutions. *Nature Reviews Drug Discovery* **2021**, *20* (8), 629-651. DOI: 10.1038/s41573-021-00219-z.
(8) Kaminski, M. M.; Abudayyeh, O. O.; Gootenberg, J. S.; Zhang, F.; Collins, J. J. CRISPR-based diagnostics. *Nature Biomedical Engineering* **2021**, *5* (7), 643-656. DOI: 10.1038/s41551-021-00760-7.

(9) Rühle, J.; Klemt, I.; Abakumova, T.; Sergeeva, O.; Vetosheva, P.; Zatsepin, T.; Mokhir, A. Reactive oxygen species-responsive RNA interference. *Chemical Communications* **2022**, *58* (27), 4388-4391, 10.1039/D2CC00651K. DOI: 10.1039/D2CC00651K.
(10) Spitale, R. C.; Flynn, R. A.; Zhang, Q. C.; Crisalli, P.; Lee, B.; Jung, J.-W.; Kuchelmeister, H. Y.; Batista, P. J.; Torre, E. A.; Kool, E. T.; et al. Structural imprints in vivo decode RNA regulatory mechanisms. *Nature* **2015**, *519* (7544), 486-490. DOI: 10.1038/nature14263.
(11) Smola, M. J.; Weeks, K. M. In-cell RNA structure probing with SHAPE-MaP. *Nature Protocols* **2018**, *13* (6), 1181-1195. DOI: 10.1038/nprot.2018.010.
(12) Mamot, A.; Sikorski, P. J.; Siekierska, A.; de Witte, P.; Kowalska, J.; Jemielity, J. Ethylenediamine derivatives efficiently react with oxidized RNA 3′ ends providing access to mono and dually labelled RNA probes for enzymatic assays and in vivo translation. *Nucleic Acids Research* **2022**, *50* (1), e3-e3. DOI: 10.1093/nar/gkab867 (acccessed 3/14/2024).
(13) Shioi, R.; Xiao, L.; Kool, E. T. Aqueous Activation of RNA 2′-OH for Conjugation with Amines and Thiols. *Bioconjugate Chemistry* **2024**, *35* (1), 43-50. DOI: 10.1021/acs.bioconjchem.3c00370.
(14) Habibian, M.; McKinlay, C.; Blake, T. R.; Kietrys, A. M.; Waymouth, R. M.; Wender, P. A.; Kool, E. T. Reversible RNA acylation for control of CRISPR–Cas9 gene editing. *Chemical Science* **2020**, *11* (4), 1011-1016, 10.1039/C9SC03639C. DOI: 10.1039/C9SC03639C.
(15) Park, H. S.; Kietrys, A. M.; Kool, E. T. Simple alkanoyl acylating agents for reversible RNA functionalization and control. *Chemical Communications* **2019**, *55* (35), 5135-5138, 10.1039/C9CC01598A. DOI: 10.1039/C9CC01598A.
(16) Kadina, A.; Kietrys, A. M.; Kool, E. T. RNA Cloaking by Reversible Acylation. *Angewandte Chemie International Edition* **2018**, *57* (12), 3059-3063. DOI: https://doi.org/10.1002/anie.201708696 (acccessed 2024/03/13).
(17) Velema, W. A.; Kietrys, A. M.; Kool, E. T. RNA Control by Photoreversible Acylation. *Journal of the American Chemical Society* **2018**, *140* (10), 3491-3495. DOI: 10.1021/jacs.7b12408.
(18) Xiao, L.; Fang, L.; Kool, E. T. 2′-OH as a universal handle for studying intracellular RNAs. *Cell Chemical Biology* **2024**, *31* (1), 110-124. DOI: 10.1016/j.chembiol.2023.10.022 (acccessed 2024/03/13).
(19) Fang, L.; Xiao, L.; Jun, Y. W.; Onishi, Y.; Kool, E. T. Reversible 2′-OH acylation enhances RNA stability. *Nature Chemistry* **2023**, *15* (9), 1296-1305. DOI: 10.1038/s41557-023-01246-6.
(20) Park, H. S.; Jash, B.; Xiao, L.; Jun, Y. W.; Kool, E. T. Control of RNA with quinone methide reversible acylating reagents. *Organic & Biomolecular Chemistry* **2021**, *19* (38), 8367-8376, 10.1039/D1OB01713F. DOI: 10.1039/D1OB01713F.
(21) Han, J.; Han, M. S.; Tung, C.-H. A fluorogenic probe for β-galactosidase activity imaging in living cells. *Molecular BioSystems* **2013**, *9* (12), 3001-3008, 10.1039/C3MB70269C. DOI: 10.1039/C3MB70269C.
(22) Shirangi, M.; Najafi, M.; Rijkers, D. T. S.; Kok, R. J.; Hennink, W. E.; van Nostrum, C. F. Inhibition of Octreotide Acylation Inside PLGA Microspheres by Derivatization of the Amines of the Peptide with a Self-Immolative Protecting Group. *Bioconjugate Chemistry* **2016**, *27* (3), 576-585. DOI: 10.1021/acs.bioconjchem.5b00598.
(23) Duan, W.; Ji, S.; Guan, Y.; Mu, X.; Fang, S.; Lu, Y.; Zhou, X.; Sun, J.; Li, Z. Esterase-Responsive Polypeptide Vesicles as Fast-Response and Sustained-Release Nanocompartments for Fibroblast-Exempt Drug Delivery. *Biomacromolecules* **2020**, *21* (12), 5093-5103. DOI: 10.1021/acs.biomac.0c01251.

(24) Rafeeq, H.; Hussain, A.; Shabbir, S.; Ali, S.; Bilal, M.; Sher, F.; Iqbal, H. M. N. Esterases as emerging biocatalysts: Mechanistic insights, genomic and metagenomic, immobilization, and biotechnological applications. *Biotechnology and Applied Biochemistry* **2022**, *69* (5), 2176-2194. DOI: https://doi.org/10.1002/bab.2277 (acccessed 2024/06/16).
(25) Liang, P.; Zhang, Y.; Schmidt, B. F.; Ballou, B.; Qian, W.; Dong, Z.; Wu, J.; Wang, L.; Bruchez, M. P.; Dong, X. Esterase-Activated, pH-Responsive, and Genetically Targetable Nano-Prodrug for Cancer Cell Photo-Ablation. *Small* **2023**, *19* (19), 2207535. DOI: https://doi.org/10.1002/smll.202207535 (acccessed 2024/06/16).
(26) Zhu, X.; Zhao, T.; Nie, Z.; Miao, Z.; Liu, Y.; Yao, S. Nitrogen-doped carbon nanoparticle modulated turn-on fluorescent probes for histidine detection and its imaging in living cells. *Nanoscale* **2016**, *8* (4), 2205-2211, 10.1039/C5NR07826A. DOI: 10.1039/C5NR07826A.
(27) Liu, L.; Zhang, L.; Tao, M.; Wang, M.; Dong, L.; Hai, Z. An esterase-activatable curcumin prodrug for tumor-targeting therapy. *Chemical Communications* **2022**, *58* (96), 13329-13332, 10.1039/D2CC03952D. DOI: 10.1039/D2CC03952D.
(28) Dong, H.; Pang, L.; Cong, H.; Shen, Y.; Yu, B. Application and design of esterase-responsive nanoparticles for cancer therapy. *Drug Delivery* **2019**, *26* (1), 416-432. DOI: 10.1080/10717544.2019.1588424.
(29) Gu, X.; Yang, K.; Li, S.; Mei, J.; He, X.-P.; Chen, W.; Hua, J. An esterase-activated diketopyrrolopyrrole-based theranostic prodrug for precise pyroptosis and synergistic chemo-photodynamic therapy of pancreatic cancer†. *Materials Chemistry Frontiers* **2024**, 10.1039/D4QM00052H. DOI: 10.1039/D4QM00052H.
(30) Pohanka, M. Cholinesterases, a target of pharmacology and toxicology. *Biomed Pap Med Fac Univ Palacky Olomouc Czech Repub* **2011**, *155* (3), 219-229. DOI: 10.5507/bp.2011.036 From NLM.
(31) Sharma, K. Cholinesterase inhibitors as Alzheimer's therapeutics (Review). *Mol Med Rep* **2019**, *20* (2), 1479-1487. DOI: 10.3892/mmr.2019.10374.
(32) Kirsch, J. F.; Jencks, W. P. Base Catalysis of Imidazole Catalysis of Ester Hydrolysis. *Journal of the American Chemical Society* **1964**, *86* (5), 833-837. DOI: 10.1021/ja01059a018.
(33) Filonov, G. S.; Moon, J. D.; Svensen, N.; Jaffrey, S. R. Broccoli: Rapid Selection of an RNA Mimic of Green Fluorescent Protein by Fluorescence-Based Selection and Directed Evolution. *Journal of the American Chemical Society* **2014**, *136* (46), 16299-16308. DOI: 10.1021/ja508478x.
(34) Ouellet, J. RNA Fluorescence with Light-Up Aptamers. *Frontiers in Chemistry* **2016**, *4*, Review. DOI: 10.3389/fchem.2016.00029.
(35) Elsner, M. Single-stranded siRNAs for in vivo gene silencing. *Nature Biotechnology* **2012**, *30* (11), 1063-1063. DOI: 10.1038/nbt.2413.
(36) Allison, S. J.; Milner, J. RNA Interference by Single- and Double-stranded siRNA With a DNA Extension Containing a 3′ Nuclease-resistant Mini-hairpin Structure. *Molecular Therapy - Nucleic Acids* **2014**, *3*. DOI: 10.1038/mtna.2013.68 (acccessed 2024/03/17).
(37) Moradian, H.; Lendlein, A.; Gossen, M. Strategies for simultaneous and successive delivery of RNA. *Journal of Molecular Medicine* **2020**, *98* (12), 1767-1779. DOI: 10.1007/s00109-020-01956-1.
(38) Knutson, S. D.; Sanford, A. A.; Swenson, C. S.; Korn, M. M.; Manuel, B. A.; Heemstra, J. M. Thermoreversible Control of Nucleic Acid Structure and Function with Glyoxal Caging. *Journal of the American Chemical Society* **2020**, *142* (41), 17766-17781. DOI: 10.1021/jacs.0c08996.
(39) Paunovska, K.; Loughrey, D.; Dahlman, J. E. Drug delivery systems for RNA therapeutics. *Nature Reviews Genetics* **2022**, *23* (5), 265-280. DOI: 10.1038/s41576-021-00439-4.

(40) Dowdy, S. F. Endosomal escape of RNA therapeutics: How do we solve this rate-limiting problem? *RNA* **2023**, *29* (4), 396-401. DOI: 10.1261/rna.079507.122.
(41) Lam, J. K. W.; Chow, M. Y. T.; Zhang, Y.; Leung, S. W. S. siRNA Versus miRNA as Therapeutics for Gene Silencing. *Molecular Therapy - Nucleic Acids* **2015**, *4*. DOI: 10.1038/mtna.2015.23 (acccessed 2024/08/22).
(42) Guo, J.; Chen, S.; Onishi, Y.; Shi, Q.; Song, Y.; Mei, H.; Chen, L.; Kool, E. T.; Zhu, R. Y. RNA Control via Redox-Responsive Acylation. *Angew Chem Int Ed Engl* **2024**, *63* (21), e202402178. DOI: 10.1002/anie.202402178 From NLM.
(43) Tian, X.; Yan, F.; Zheng, J.; Cui, X.; Feng, L.; Li, S.; Jin, L.; James, T. D.; Ma, X. Endoplasmic Reticulum Targeting Ratiometric Fluorescent Probe for Carboxylesterase 2 Detection in Drug-Induced Acute Liver Injury. *Analytical Chemistry* **2019**, *91* (24), 15840-15845. DOI: 10.1021/acs.analchem.9b04189.
(44) Yang, B.; Ding, X.; Zhang, Z.; Li, J.; Fan, S.; Lai, J.; Su, R.; Wang, X.; Wang, B. Visualization of production and remediation of acetaminophen-induced liver injury by a carboxylesterase-2 enzyme-activatable near-infrared fluorescent probe. *Talanta* **2024**, *269*, 125418. DOI: https://doi.org/10.1016/j.talanta.2023.125418.
(45) Xiao, D.; Yang, D.; Guo, L.; Lu, W.; Charpentier, M.; Yan, B. Regulation of carboxylesterase-2 expression by p53 family proteins and enhanced anti-cancer activities among 5-fluorouracil, irinotecan and doxazolidine prodrug. *British Journal of Pharmacology* **2013**, *168* (8), 1989-1999. DOI: https://doi.org/10.1111/bph.12125 (acccessed 2024/04/27).
(46) Zhang, W.; Qi, C.; Wang, X.; Fu, Z.; Zhang, J.; Zhou, Y.; Wang, Y. An ultrasensitive and selective near-infrared fluorescent probe for tracking carboxylesterases with large Stokes shift in living cells and mice. *Spectrochimica Acta Part A: Molecular and Biomolecular Spectroscopy* **2024**, *308*, 123708. DOI: https://doi.org/10.1016/j.saa.2023.123708.
(47) Zhang, J.; Peng, Y.; Li, Y.; Wang, N.; Chai, Y.; Qin, C.; Wang, X.; Liu, S.; Zhou, Y.; Zhang, X.; et al. Development of a near-infrared fluorescent probe with large Stokes shift for carboxylesterases detection and its application in living systems. *Dyes and Pigments* **2022**, *198*, 109993. DOI: https://doi.org/10.1016/j.dyepig.2021.109993.
(48) Lin, X.; Liu, M.; Yi, Q.; Zhou, Y.; Su, J.; Qing, B.; Lu, Y.; Pu, C.; Lan, W.; Zou, L.; et al. Design, synthesis, and evaluation of a carboxylesterase detection probe with therapeutic effects. *Talanta* **2024**, *274*, 126060. DOI: https://doi.org/10.1016/j.talanta.2024.126060.
(49) Liu, S.-Y.; Qu, R.-Y.; Li, R.-R.; Yan, Y.-C.; Sun, Y.; Yang, W.-C.; Yang, G.-F. An Activity-Based Fluorogenic Probe Enables Cellular and in Vivo Profiling of Carboxylesterase Isozymes. *Analytical Chemistry* **2020**, *92* (13), 9205-9213. DOI: 10.1021/acs.analchem.0c01554.
(50) Chen, Y.; Liu, W.; Zhang, B.; Suo, Z.; Xing, F.; Feng, L. Sensitive and reversible perylene derivative-based fluorescent probe for acetylcholinesterase activity monitoring and its inhibitor. *Analytical Biochemistry* **2020**, *607*, 113835. DOI: https://doi.org/10.1016/j.ab.2020.113835.
(51) Ma, J.; Lu, X.; Zhai, H.; Li, Q.; Qiao, L.; Guo, Y. Rational design of a near-infrared fluorescence probe for highly selective sensing butyrylcholinesterase (BChE) and its bioimaging applications in living cell. *Talanta* **2020**, *219*, 121278. DOI: https://doi.org/10.1016/j.talanta.2020.121278.
(52) Fortibui, M. M.; Jang, M.; Lee, S.; Ryoo, I.-J.; Ahn, J. S.; Ko, S.-K.; Kim, J. Near-Infrared Fluorescence Probe for Specific Detection of Acetylcholinesterase and Imaging in Live Cells and Zebrafish. *ACS Applied Bio Materials* **2022**, *5* (5), 2232-2239. DOI: 10.1021/acsabm.2c00084.

(53) Shi, Y.; Zhen, X.; Zhang, Y.; Li, Y.; Koo, S.; Saiding, Q.; Kong, N.; Liu, G.; Chen, W.; Tao, W. Chemically Modified Platforms for Better RNA Therapeutics. *Chemical Reviews* **2024**, *124* (3), 929-1033. DOI: 10.1021/acs.chemrev.3c00611.
(54) Shiraishi, K.; Yokoyama, M. Toxicity and immunogenicity concerns related to PEGylated-micelle carrier systems: a review. *Science and Technology of Advanced Materials* **2019**, *20* (1), 324-336. DOI: 10.1080/14686996.2019.1590126.
(55) Deeyaa, B. D.; Rokita, S. E. Migratory ability of quinone methide-generating acridine conjugates in DNA. *Organic & Biomolecular Chemistry* **2020**, *18* (8), 1671-1678, 10.1039/D0OB00081G. DOI: 10.1039/D0OB00081G.
(56) Zhou, B.; Wang, B.; Bai, M.; Dong, M.; Tang, X. Fluorescent probe for highly selective detection of cysteine in living cells. *Spectrochimica Acta Part A: Molecular and Biomolecular Spectroscopy* **2023**, *294*, 122523. DOI: https://doi.org/10.1016/j.saa.2023.122523.